Differences in sympathetic neuroeffector transmission to rat mesenteric arteries and veins as probed by *in vitro* continuous amperometry and video imaging

Jinwoo Park[1], James J. Galligan[2], Gregory D. Fink[2] and Greg M. Swain[1]

[1]*Department of Chemistry and the Neuroscience Program, Michigan State University, East Lansing, MI 48824, USA*
[2]*Department of Pharmacology and Toxicology and the Neuroscience Program, Michigan State University, East Lansing, MI 48824, USA*

As arteries are resistance blood vessels while veins perform a capacitance function, it might be expected that sympathetic neural control of arteries and veins would differ. The function of sympathetic nerves supplying mesenteric arteries (MA) and veins (MV) in rats was investigated using *in vitro* continuous amperometry with a carbon fibre microelectrode and video imaging. We simultaneously measured noradrenaline (NA) overflow at the blood vessel adventitial surface and vasoconstriction evoked by electrical stimulation of perivascular sympathetic nerves. Sympathetic nerve arrangement was studied using glyoxylic acid-induced fluorescence of NA. We found that: (i) there were significant differences between MA and MV in the arrangement of sympathetic nerves; (ii) frequency–response curves for NA overflow and vasoconstriction for MV were left-shifted compared to MA; (iii) the P2X receptor antagonist, pyridoxal-phosphate-6-azophenyl-2′,4′-disulphonic acid (PPADS, 10 μM), reduced constrictions in MA but not in MV while the α_1-adrenergic receptor antagonist, prazosin (0.1 μM), blocked constrictions in MV but not in MA; (iv) NA overflow for MA was enhanced by the α_2-adrenergic receptor antagonist, yohimbine (1.0 μM), and attenuated by the α_2-adrenergic receptor agonist, UK 14,304 (1.0 μM), while yohimbine and UK 14,304 had little effect in MV; (v) cocaine (10 μM) produced larger increases in NA overflow in MA than in MV; (vi) UK 14,304 constricted MV but not MA while yohimbine reduced constrictions in MV but not MA. We conclude that there are fundamental differences in sympathetic neuroeffector mechanisms in MA and MV, which are likely to contribute to their different haemodynamic functions.

(Received 11 April 2007; accepted after revision 29 August 2007; first published online 30 August 2007)
Corresponding author G. M. Swain: Department of Chemistry and the Neuroscience Program, Michigan State University, East Lansing, MI 48824, USA. Email: swain@chemistry.msu.edu

Sympathetic nerve activity plays a prominent role in regulating the resistance and capacitance functions of arteries and veins, respectively. Arterial blood vessels distribute oxygenated blood to tissues with diverse functions and rapidly changing oxygen requirements. Therefore, arterial directed sympathetic activity must allow precise moment-to-moment control of regional blood flow and systemic arterial pressure (Segal, 2000). On the other hand, veins function as a blood reservoir. Shifting blood from systemic veins to arteries in response to orthostatic or other physiological disturbances requires a rapid and sustained sympathetic activation of venous smooth muscle (Tani *et al.* 2000). Highly innervated veins of the splanchnic circulation are particularly important contributors to this redistributive function of the venous system (Daugirdas, 2001; Kreulen, 2003*a*). The nervous system may generate the required differences in control dynamics using differentiated patterns and/or levels of nerve firing to arteries and veins. Differential control may also occur at the neuroeffector junction. In fact, veins differ significantly from arteries in their contractile and electrical responses to sympathetic nerve stimulation or to drugs that mimic the activity of sympathetic nerves (Kreulen, 1986; Hottenstein & Kreulen, 1987; Bobalova & Mutafova-Yambolieva, 2001). One reason for these differences is that arteries and veins may be innervated by distinct sympathetic neurons and these neurons may communicate using different neurotransmitters. Adenosine 5′-triphosphate (ATP) and noradrenaline (NA) are neurotransmitters released by sympathetic nerves supplying small (~250 μm) mesenteric arteries while NA is the primary vasoconstrictor released by perivenous nerves (Hottenstein & Kreulen, 1987; Hirst & Jobling, 1989; Stjarne *et al.* 1994; Westfall *et al.* 1996).

 DOI: 10.1113/jphysiol.2007.134338

Sympathetic neuroeffector transmission in arteries and veins may differ because there are distinctive mechanisms regulating neurotransmitter release and clearance. Continuous amperometry with a microelectrode has been used to examine neurotransmission in the peripheral nervous system. With this method, movement of an electroactive neurotransmitter from local neuroeffector junctions is measured as an oxidation current that is proportional to the concentration at the blood vessel surface. This technique provides time-dependent information on the local concentration of a redox-active molecule at the blood vessel surface that results from release at nearby varicosities. The measured current corresponds to efflux from multiple release sites nearby the microlectrode and not release from a single neuroeffector junction. For sympathetic nerves, NA is the electroactive neurotransmitter monitored. Electrochemical methods have been used to study NA release from sympathetic nerve endings in rat tail and mesenteric arteries (Mermet *et al.* 1990; Gonon *et al.* 1993; Gonon, 1995; Dunn *et al.* 1999; Dugast *et al.* 2002; Brock & Tan, 2004; Teschemacher, 2005; Yavich *et al.* 2005). NA overflow from perivascular nerves can be oxidatively detected in the presence of other cotransmitters, including ATP and neuropeptide Y (NPY), because the latter two compounds are electroinactive. Therefore, electrochemical methods are quite useful for mechanistic studies of endogenous NA release and clearance in vascular tissues, but have not yet been applied to the study of veins.

In the present work, continuous amperometry was used to record NA overflow *in vitro* at the adventitial surface of isolated rat mesenteric artery (MA) and vein (MV) preparations in response to focal electrical stimulation. Using a carbon fibre microelectrode, oxidation current measurements were made that provided information regarding the temporal change in NA concentration at the blood vessel surface in response to a stimulus. This concentration is determined by complex and highly regulated mechanisms effecting both transmitter release and clearance. Pharmacological methods were used to investigate some of these mechanisms. Video imaging was used to monitor blood vessel constriction simultaneously with changes in the NA oxidation current. The combined measurement of NA and vessel diameter provides detailed information on the time-dependent relationship between vascular contraction and NA concentration at the blood vessel surface. We used these techniques to test the hypothesis that there are fundamental differences in the dynamics of sympathetic neuroeffector transmission in mesenteric arteries and veins.

Methods

Carbon fibre microelectrode preparation

Heat-treated (3000°C) pitch-base type carbon fibres (formerly AVCO Specialty Materials, Inc., Lowell, MA, USA) having a nominal diameter of 35 μm were used. Each carbon fibre was attached to a longer copper wire with conductive silver epoxy. The carbon fibre–copper wire assembly was then inserted into a polypropylene pipette tip and the tapered end was carefully heated in a micropipette puller. This softened the polypropylene and caused it to flow over the carbon fibre surface, thus insulating the electrode (Chow *et al.* 1992; Zhou & Misler, 1996; Park *et al.* 2005). The resulting microelectrode possessed a cylindrical architecture with an exposed length of *ca* 500 μm (geometric area $= 5 \times 10^{-4}$ cm^2). Electrodes insulated with polypropylene are generally non-toxic to tissue and chemically resistant to the isopropyl alcohol (IPA) used for electrode cleaning (Ranganathan *et al.* 1999). The carbon fibre was used *in vitro* without any electrochemical pretreatment for activation or Nafion coating for fouling protection (Stamford, 1986). We previously reported that a 25% response (i.e. sensitivity) attenuation in the measured oxidation current for NA is typical for a bare carbon fibre during the first 2 h of exposure to a mesenteric blood vessel, if most of the adipose and connective tissue is first removed. Little change in the response occurs thereafter (Park *et al.* 2005). In the present work, a new carbon fibre was exposed to the tissue and the flowing physiological buffer for a period of about 2 h in order to equilibrate the tissue and to stabilize the response prior to the start of a series of measurements. Recent work by our group has shown that diamond microelectrode offers advantages over traditional carbon fibre for *in vitro* electrochemical measurements of NA in terms of response sensitivity, reproducibility and stability (Park *et al.* 2005, 2006*a*,*b*). However, we were unable to make use of this microelectrode in this work because some of the drugs employed were oxidatively detected at the positive potential used to measure NA. This was not the case for carbon fibre as NA was detected at a less positive potential, a value at which the drugs were non-responsive.

Preparation of mesenteric vessels for *in vitro* electrochemical and contractile measurements

The Institutional Animal Care and Use Committee at Michigan State University approved all animal handling and use procedures. The male Sprague–Dawley rats (380–430 g, Charles River Inc, Portage, MI, USA) used in these studies were killed with a lethal pentobarbital injection (50 mg kg^{-1}, I.P.). The abdomen was then opened and the small intestine was carefully removed and placed in an oxygenated (95% O_2, 5% CO_2) Krebs buffer solution of the following composition: 117 mM NaCl, 4.7 mM KCl, 2.5 mM $CaCl_2$, 1.2 mM $MgCl_2$, 25 mM $NaHCO_3$, 1.2 mM NaH_2PO_4, and 11 mM glucose. A section of the mesentery close to the ileal wall was carefully cut free from the intestine and transferred to a small silicone elastomer-lined (Sylgard 184, Dow Corning)

Teflon bath (4.8 ml volume) where it was gently stretched and pinned flat. Secondary or tertiary arteries and veins (180–330 μm outer diameter) were then isolated for *in vitro* study by carefully cutting away the surrounding adipose and connective tissues under a dissecting microscope. The bath was mounted on the stage of an inverted microscope (Olympus CX41, USA) and superfused continuously with 37°C Krebs solution, pH 7.4, at a flow rate of 5–6 ml min^{-1}. The solution flow was controlled by a peristaltic pump (Masterflex, Cole Parmer, USA).

Prior to use, the carbon fibre microelectrode was cleaned by soaking in distilled isopropyl alcohol (IPA) for at least 15 min (Ranganathan *et al.* 1999). The microelectrode was then affixed to a micromanipulator (MP-1, Narishige Instruments, Japan), which enabled its reproducible positioning against the side of a MA or MV. The cylindrical portion of the microelectrode was positioned alongside the vessel so that the NA flux from nearby release sites was sensed by most of the electrode surface. This positioning allowed the microelectrode to move in conjunction with the blood vessel as it contracted and relaxed, thus enabling measurement of NA at the blood vessel surface with an unchanging electrode-blood vessel distance. We confirmed this by measuring the NA oxidation current elicited by electrical stimulation in the presence and absence of the P2X antagonist, PPADS, and the α_1 antagonist, prazosin, which together abolished arterial constriction. The oxidation currents measured were the same with and without the drugs. The microelectrode and tissue preparation were positioned in the centre of the bath, equidistant from the inlet and outlet solution ports. A platinum wire counter and a commercial 'no leak' Ag–AgCl (3 M KCl, model EE009, Cypress Systems Inc., USA) reference electrode were also mounted in the bath to complete the electrochemical cell. All electrochemical measurements were made with an Omni 90 analog potentiostat (Cypress Systems Inc.), an analog-to-digital converter (Labmaster 125) and a computer running Axotape software (version 2.0, Axon Instruments, Union City, CA, USA). Continuous amperometric *i–t* curves were recorded at a detection potential of 400 mV. At this potential, NA is oxidized at a mass-transfer limited rate. The analog voltage output from the potentiostat, a value that reflects the current flowing through the working electrode, was low-pass filtered at a time constant of 200 ms (5 Hz) before being digitized using an A/D converter at a sampling rate of 100 Hz. The data were then stored on a computer for further processing. All measurements were made in unpressurized blood vessels.

Focal stimulation of perivascular nerves

Short trains of electrical stimulation were used to trigger NA release. Perivascular nerves were stimulated using a bipolar focal stimulating electrode positioned along the surface of the blood vessel at a distance of *ca* 200 μm from the carbon fibre. This positioning minimized stimulus artifact in the current recordings. The focal stimulating electrode consisted of two AgCl-coated Ag wires inserted into a double-barrelled capillary glass (tip diameter = 180 μm). The wires were connected to a stimulus isolation unit and a Grass Instruments stimulator (S88, Quincy, MA, USA). Trains of 60 stimuli (0.3 ms pulse width, 30–70 V) at frequencies ranging between 0.5 and 20 Hz were used (Park *et al.* 2006*a*,*b*) to evoke neurotransmitter release.

Video monitoring of vasoconstriction

The output of a black–white video CCD camera (Hitachi KP-111) attached to the inverted microscope was fed to a frame grabber card (Picolo, Euresys Inc., TX, USA) mounted in a personal computer. Video images were analysed real time using Diamtrak edge-tracking software (version 3.5, http://www.diamtrak.com), which tracks the distance between the outer edges of the blood vessel in the observation field. Changes in blood vessel diameter of 1 μm could be resolved. The digitized signal was converted to an analog signal (DAC-02 board, Keithley Metrabyte, Tauton, MA, USA) for subsequent processing by an analog-to-digital converter (Labmaster 125) and analysis in a second computer running Axotape for a permanent recording of blood vessel diameter as function of time. Analog signals were sampled at 100 Hz and data were stored on the computer's hard drive for subsequent analysis and display.

Drug application

All chemicals and drugs were reagent-grade quality, or better, and were used without additional purification. Ultrapure water (distilled, deionized, and filtered over activated carbon, 17–18 MΩ, Barnstead E-Pure System) was used for all solution preparation and cleaning. Drugs were added to the superfusing Krebs solution; it took *ca* 2 min for them to reach the tissue and they were applied for 20 min prior to assessing their effects on nerve-mediated responses. Drugs were obtained from Sigma-Aldrich Chemical Company (St Louis, MO, USA).

Glyoxylic acid fluorescence histochemistry

Second- or third-order veins and arteries from the ileal mesentery were isolated by carefully cutting away the surrounding adipose and connective tissues. Red blood cells were flushed out of the blood vessel lumen with phosphate buffer (0.1 M, pH 7.2) using a 30-ga hypodermic needle and syringe, and tissues were cut to 1 cm lengths.

For these experiments, we used 20 MA and MV segments from five rats. Catecholamine fluorescence was revealed after incubating tissues in a 2% glyoxylic acid–0.2 M phosphate buffer (pH 7.0) solution for 5 min at room temperature. The blood vessels were then stretched onto glass slides and heated at 80°C for 5 min. Preparations were mounted in mineral oil and observed using a fluorescence microscope (Nikon Eclipse TE 2000-U) equipped with a filter set, UV2E/C (excitation filter, 340–380 nm and emission, 435–485 nm).

Data analysis

Analysis of the current (i)–t and diameter–t profiles was performed using Clampfit 8.1 as part of the pCLAMP 8.1 software package (Axon Instruments). Mean values were compared by using Student's paired t test (GraphPad Software, San Diego, CA, USA). $P < 0.05$ was regarded as statistically significant. Data are reported as mean ± standard error of the mean (S.E.M.) with 'n' values indicating the number of rats from which the data were obtained. MA and MV constrictions are expressed as a percentage of the initial resting diameter (in μm) of the blood vessel. For nerve stimulation frequency–response curves, the half-maximal effective stimulation frequency (S_{50}) and maximum constriction (E_{max}) were calculated from curves obtained in individual tissues using the following function:

$$Y = E_{max} X / (S_{50} + X)$$

Where X is the stimulation frequency tested and Y is the peak response amplitude.

Results

Distribution of sympathetic nerve fibres associated with MA and MV

Glyoxylic acid (GA) reacts with NA to form an intensely fluorescent 2-carboxymethyl-dihydroisoquinoline derivative (Bjorklund *et al.* 1972). The distribution of GA-induced fluorescence of neuronal stores of NA was used to assess the disposition of periarterial and perivenous sympathetic nerves. GA-induced fluorescence revealed a network of varicose nerve fibres around MA and MV (Fig. 1*A* and *B*). The periarterial nerve plexus

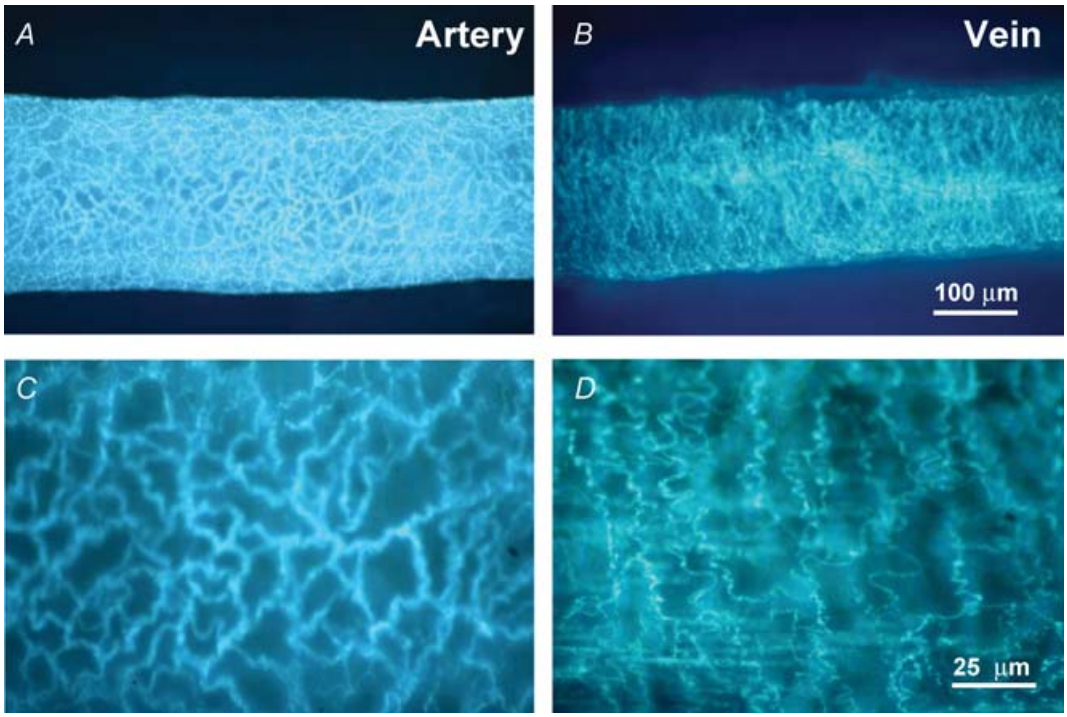

Figure 1. Glyoxylic acid-induced fluorescence of catecholamines in perivascular sympathetic nerves
A and *B* show low magnification (100×) images of sympathetic nerves while *C* and *D* show high magnification images (400×). The nerve plexus in arteries has a mesh-like arrangement of nerve fibres that are orientated along both the longitudinal and circular axis of the blood vessel (*C*). The plexus in veins has a selective circular arrangement with very few fibres orientated along the longitudinal axis of the blood vessel (*D*).

consisted of bundles of several axons arranged in a net-like manner. The perivenous plexus was less dense than in arteries and consisted of individual varicose axons largely orientated circumferentially around the vessel. Higher magnification images clearly reveal the differential nerve arrangement (Figs 1*C* and *D*). The difference in periarterial and perivenous sympathetic nerve arrangement was quantified by counting the number of nerve fibres crossing horizontal (longitudinal axis) and vertical (radial axis) grids superimposed on a vessel image (400× magnification). The number of vertical and horizontal fibre crossings was similar in MA (vertical $= 9.7 \pm 1.2$, horizontal $= 9.6 \pm 1.2$, $n = 5$), whereas there were fewer horizontal than vertical crossings in MV (horizontal $= 3.6 \pm 0.4$, vertical $= 6.8 \pm 0.9$, $n = 5$; $P < 0.05$). In addition, the number of vertical crossings in MV was significantly less than in MA ($P < 0.05$).

NA oxidation currents and constriction in MA and MV

The oxidation current measured at 400 mV reflects the concentration of endogenous NA at the blood vessel surface in the vicinity of the recording microelectrode (Park *et al.* 2005, 2006*a*,*b*). This time-dependent concentration is the net result of release from multiple varicosities near the microelectrode, clearance by neuronal reuptake, and diffusional and convective mass transport away from the release sites, the latter due to the fluid dynamics in the bath. Preparations were discarded for which the electrically evoked oxidation current or constriction were not blocked by tetrodotoxin (TTX, 0.3 μM). Several locations on a blood vessel were probed for NA oxidation currents in order to find one that yielded a 'large' current (i.e. hot spot). Finding such a spot was more difficult in MV and this is consistent with the differential arrangement of sympathetic nerve fibres revealed in Fig. 1. Sites yielding the largest oxidation current were then selected for comparative studies of perivenous and periarterial nerves. Measurable NA release was only evoked by trains of electrical stimuli (see methods section) and not by a single pulse stimulation.

The same trains of electrical stimuli produced frequency-dependent constrictions of MA and MV with NA oxidation currents and constriction being detected at a lower threshold frequency in MV (0.5 and 0.2 Hz, respectively) than in MA (1 and 0.5 Hz, respectively). Figure 2*A* and *B* displays representative recordings of constriction (top) and the NA oxidation current (bottom) for MA and MV at stimulation frequencies of 3 and 20 Hz. It can be seen that at 20 Hz, both vessels constrict by

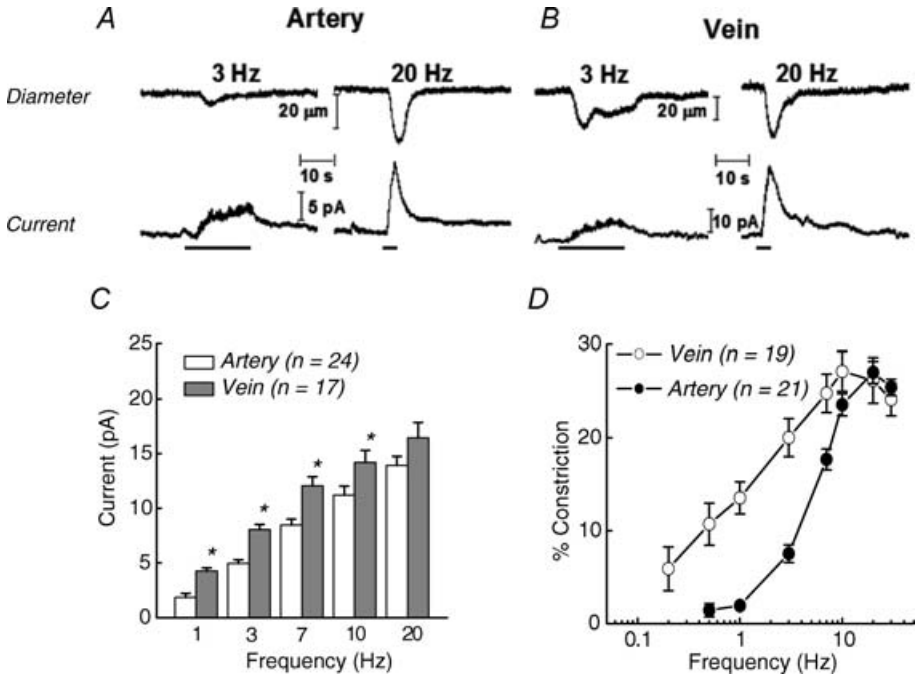

Figure 2. *In vitro* continuous amperometric measurement of NA oxidation currents and video imaging of neurogenic constriction in a MV

NA oxidation currents and neurogenic constrictions are frequency dependent. Neurogenic constrictions (top) and NA oxidation currents (bottom) caused by 3 and 20 Hz stimulus trains (60 pulses with a 0.3 ms pulse width) in a MA (*A*) and a MV (*B*). The bars under the current traces denote the period of nerve stimulation. *C* and *D*, frequency–response curves for NA-oxidation current (*C*) (*significantly different from MA, $P < 0.05$) and constriction in MA and MV (*D*). Data are means ± S.E.M.

ca 25%. The vessel constricts rapidly in response to the stimulus followed by a slow relaxation back to the resting diameter. However, 3 Hz was the threshold stimulation for a detectable arterial constriction while this frequency evoked a significant constriction of veins. At 20 Hz, the peak oxidation currents in MA and MV were 12.7 and 23.8 pA, respectively. At 3 Hz, peak currents in MA and MV were 5.1 and 9.8 pA, respectively.

Figure 2*C* and *D* contains summary plots of the oxidation currents and constrictions for MA and MV. The data demonstrate a frequency-dependent increase in the NA oxidation current and constriction for MA and MV. These data also reveal that NA oxidation currents were greater for MV than for MA and that the frequency–response curve for nerve stimulation-induced constriction in MV was left-shifted from the curve for MA. The half-maximum stimulation frequency (S_{50}) of the constriction was 1.9 ± 0.2 Hz for MV, and this value was significantly lower ($P < 0.05$) than the 4.8 ± 0.3 Hz for MA. The maximum constriction (E_{max}) was similar in MV ($28 \pm 2\%$) and MA ($31 \pm 3\%$).

Influence of PPADS and prazosin on NA oxidation current and vasoconstriction

Along with NA acting on α_1-adrenergic receptors, ATP acting at P2X purinergic receptors contributes to sympathetic neurogenic constriction of arteries in the rat mesentery (Dunn *et al.* 1999; Gitterman & Evans, 2001; Luo *et al.* 2003). In order to study the noradrenergic component of the constriction independently, the P2X receptor antagonist, PPADS (10 μM), was used to block the constricting effect of ATP. Figure 3*A* shows that PPADS did not alter the NA oxidation current elicited by 20 Hz stimulation but did substantially reduce the MA constriction. In contrast, PPADS affected neither the oxidation current nor constriction of MV (Fig. 3*B*). This result indicates that ATP largely mediates neurogenic constriction of MA while NA mediates neurogenic constriction of MV.

The α_1-adrenergic receptor antagonist, prazosin (0.1 μM), was also applied to the tissues individually and in combination with PPADS. Prazosin reduced the neurogenically mediated constriction of MA while PPADS and prazosin together totally blocked constriction without altering the NA oxidation current. In contrast, PPADS had no effect on either constriction or NA oxidation current from MV, while prazosin blocked constriction (Fig. 3*D*) but had no effect on NA oxidation current.

Quantitative determination of NA at the blood vessel surface

Determining the proportionality between the measured current and the local NA concentration is a complex issue. It is supposed that much of the electrode surface is sensing the NA overflow, so we tried to mimic this type of release by calibrating the microelectrode in the flow bath using different injected concentrations of NA. This was accomplished by introducing a NA solution through a non-metallic (combination of plastic and fused silica) needle (i.d. 250 μm, MicroFil) that was positioned at a fixed distance from the microelectrode (*ca* 10 μm, Park *et al.* 2005). Calibration was performed before and after a series of measurements at the blood vessel to verify the minimal response attenuation occurred. Oxidation currents increased proportionally with the injected NA concentration between 5 and 300 nM ($r^2 > 0.995$). The minimum detectable concentration was 5–10 nM (signal to noise ratio = 3). Based on this calibration, the maximum oxidation current elicited by a 10 Hz stimulus train corresponds to an apparent concentration between 10 and 30 nM. This value is in good agreement with values (40–120 nM) reported for the densely innervated rat artery elicited by a 5 Hz, 100 s stimulation (Mermet *et al.* 1990; Gonon *et al.* 1993). Comparison of the apparent NA concentration–constriction curves in the presence of PPADS for MA and MV indicates that MA are relatively insensitive to endogenously released NA with a maximum constriction of *ca* 7% at 20 nM (Fig. 3*C*). MV are more sensitive to endogenous NA as 20 nM caused a 3-fold greater constriction (Fig. 3*D*).

Kinetics of NA oxidation currents and neurogenic constriction in MA and MV

The kinetics of NA release and clearance, and vasoconstriction were quantitatively different in MA and MV. Figure 4 shows superimposed temporal profiles for MA and MV constriction (top) and NA oxidation current (bottom) evoked by a 20 Hz train of stimuli. The rising portion of the oxidation current reflects the kinetics of release offset by the kinetics of clearance (reuptake and mass transfer) while current decay reflects NA clearance kinetics. The representative traces illustrate that the latency for onset of constriction is shorter in MA but the rise time of constriction is more rapid in MV. The decay time for the constriction is longer in MV. There was no difference in the latency to onset of the oxidation current between MA and MV. The rise time of the current was shorter in MV but the decay time in MV was longer than that in MA. The rate of rise of the oxidation current elicited by 3 and 20 Hz stimulation in MV was significantly faster than that in MA (Fig. 5*A*). However, there were no artery–vein differences in the decay half-time of the oxidation currents (Fig. 5*B*). The rate of constriction (μm s^{-1}) for MV was more rapid than that for MA (Fig. 5*B*). The constriction duration was longer for MV than MA at both stimulation frequencies (Figs 5*C* and *D*).

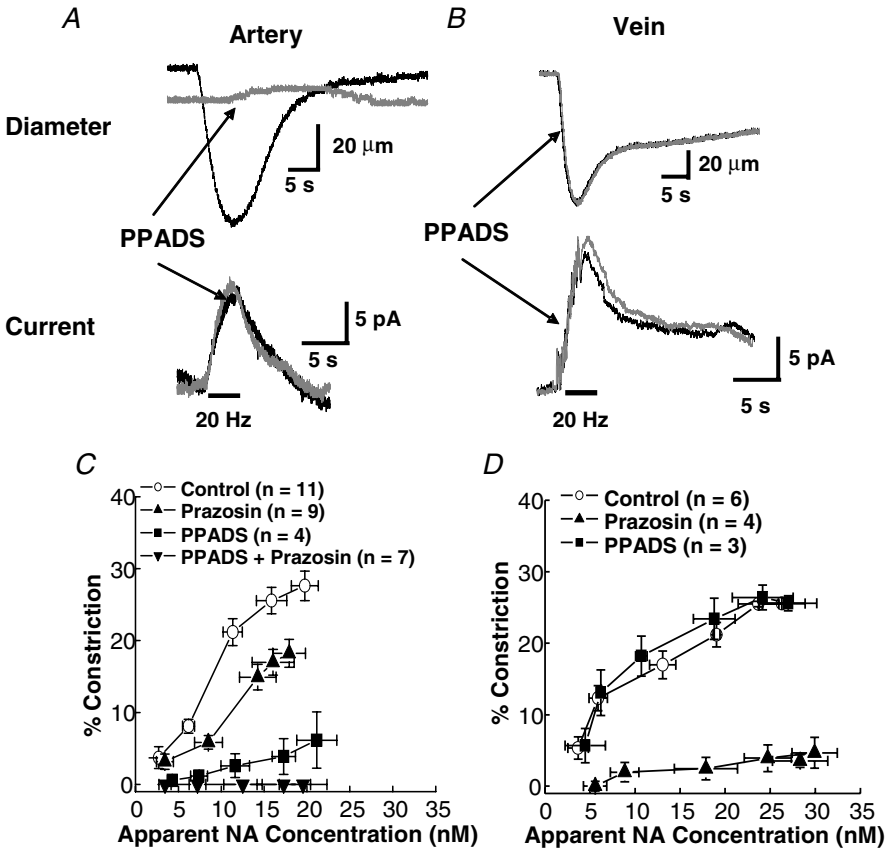

Figure 3. Contribution of α_1-adrenergic and P2X purinergic receptors to neurogenic constriction of MA and MV

A, effects of PPADS (10 μM) on neurogenic constriction (top) and NA-oxidation current caused by a 20 Hz stimulus train (60 pulses with a 0.3 ms pulse width) in a MA. PPADS blocked the constriction but not the NA oxidation current. *B*, PPADS did not alter the neurogenic constriction or NA oxidation current in a MV. *C*, apparent concentration–constriction curves for neurally released NA in MA in the absence and presence of PPADS and prazosin (0.1 μM). Peak NA oxidation currents were measured during stimulus trains (0.2–20 Hz) by converting oxidation currents to apparent NA concentrations using calibrated electrodes. The curve obtained in the presence of PPADS (square symbols) reveals the sensitivity of MA to neurally relased NA. *D*, experiments similar to 'C' except these studies were done in MV. The curve obtained in the presence of PPADS (■) reveals the sensitivity of MV to neurally relased NA. Prazosin blocked the constriction caused by nerve stimulation in MV but it did not alter the NA oxidation current (not shown). Data are means ± S.E.M.

Influence of prejunctional α_2-adrenergic receptors on NA oxidation currents and vasoconstriction

Prejunctional α_2-adrenergic autoreceptors located at the sympathetic nerve terminals are activated by NA and function to regulate its release (Langer, 1980; Stjarne *et al.* 1994; Dunn *et al.* 1999; Westfall *et al.* 2002; Brock & Tan, 2004). The influence of the α_2-adrenergic receptor antagonist, yohimbine (1.0 μM), and the agonist, UK 14,304 (1.0 μM), on NA oxidation currents and constriction of MA and MV was studied. MA constriction at 20 Hz was unchanged by yohimbine (Fig. 6*A*) while MV constriction decreased by 13%. (Fig. 6*B*). Apparently, α_2 receptors contribute to NA-induced constriction of MV. Yohimbine increased the maximum oxidation current for MA by 66% from 16.6 to 27.6 pA, whereas yohimbine increased the current for MV by only 9% from 16.1 to 17.5 pA (Fig. 6*C*). With the α_2-adrenergic autoreceptors

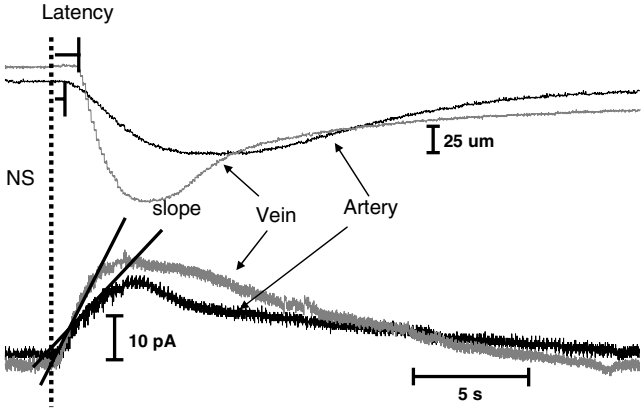

Figure 4. Kinetics of NA oxidation current and neurogenic vasoconstriction in MA and MV

Responses were evoked using a 20 Hz stimulus train (60 pulses with a 0.3 ms pulse width). The dotted line shows the onset of nerve stimulation.

blocked, NA overflow for MA was greater than that for MV at all frequencies (Fig. 6*C*). The largest increases were observed in MA and MV at the lower stimulation frequencies. Figure 6*D* shows that the elevated junctional NA concentration in the presence of yohimbine increased the contractile response for MA at frequencies up to about 7 Hz, as compared to control. Above this frequency, constriction was the same with and without the drug presumably due to saturation of postjunctional receptors. In contrast, MV constriction was unaltered by yohimbine at frequencies up to 7 Hz, above which constriction declined.

Tables 1 and 2 present a statistical analysis of the NA oxidation current and contractile response data with and without (control) yohimbine in MA and MV, respectively. In the presence of yohimbine, the rate of rise (slope) of the oxidation current increased significantly at both 3 and 20 Hz for MA, but there was no significant difference in the half-decay time or the constriction rate. The rate of rise of the current and the half-time of current decay were increased significantly in the presence of yohimbine only at 3 Hz for MV. The rate of constriction was reduced by yohimbine at both stimulation frequencies while the relaxation times were unchanged by yohimbine in MV (Table 2).

Figure 7*A* and *B* shows constrictions and oxidation currents for MA and MV in response to a 20 Hz train of stimuli with and without (control) the α_2 receptor agonist, UK 14,304. UK 14,304 decreased the oxidation current in MA by 73% from 16.5 to 4.4 pA, whereas the current for MV decreased by only 29% from 20.8 to 14.8 pA. Constrictions of MA decreased from 28 to 17% in the presence of UK 14,304 while the response for MV decreased from 28 to 13% at 20 Hz. UK 14,304 constricted MV by $15 \pm 6\%$ ($n = 6$) in the absence of any electrical stimulation, consistent with the presence of postjunctional α_2 receptors in the smooth muscle cells of MV. The plots in Fig. 7*C* show that oxidation currents were abolished in MA by UK 14,304 except at high frequencies. On the other hand, NA currents in MV were reduced less by UK 14,304.

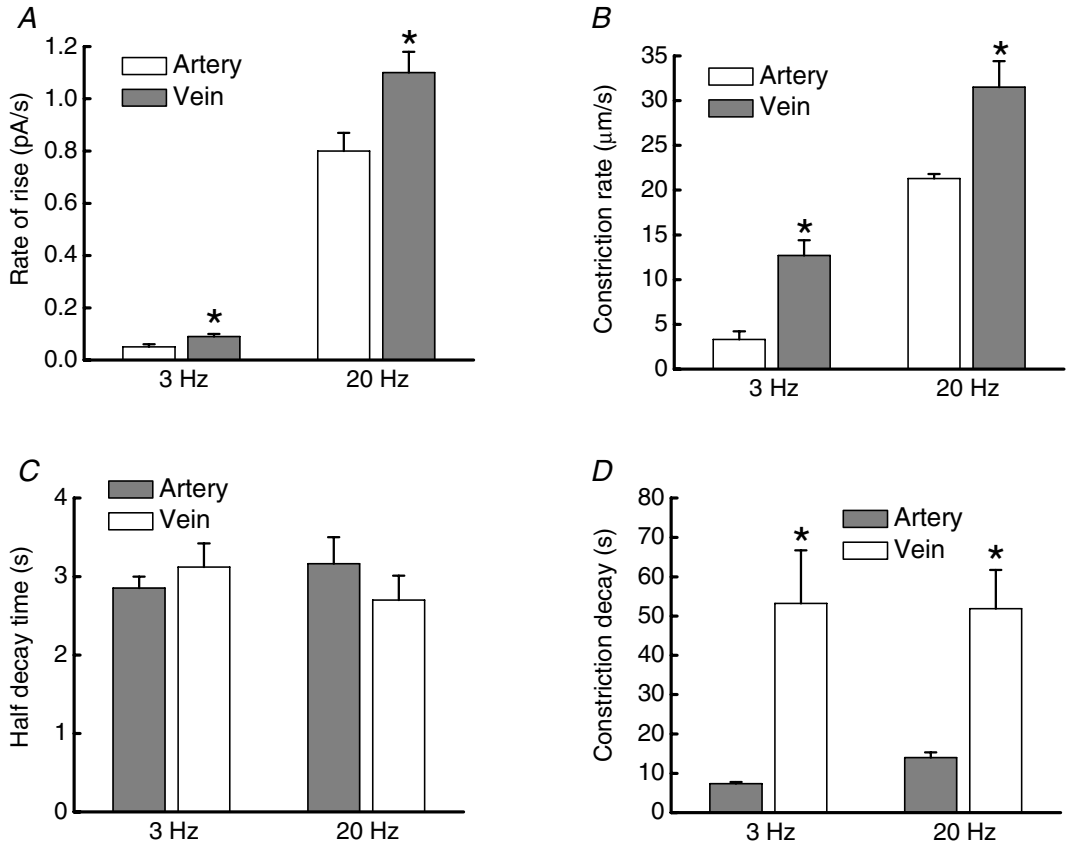

Figure 5. Comparison of the time course of NA oxidation currents and constrictions in MA and MV
A, rate of rise of the NA oxidation current is significantly faster in veins ($n = 20$) compared to arteries ($n = 10$). *B*, the rate of constriction was faster in veins compared to arteries. *C*, half-decay time of the NA oxidation current was not different in arteries and veins. Oxidation currents were evoked by 3 and 20 Hz trains of stimuli. *D*, the time to decay of constriction in veins was significantly longer than that in arteries after both 3 and 20 Hz trains of stimulation. *Significantly different from value in arteries ($P < 0.05$).

Constrictions in MA and MV were significantly reduced by UK 14,304 (Fig. 7*D*).

Influence of cocaine and yohimbine on NA oxidation currents and vasoconstriction

NA is cleared from the neuroeffector junction by the noradrenealine transporter (NET), which is blocked by cocaine (Mermet *et al.* 1990; Gonon *et al.* 1993). Figure 8*A* and *B* shows constrictions (top) and oxidation currents (bottom) for MA and MV elicited by a 20 Hz train of stimuli before (control) and after the addition of cocaine (10 μM). Cocaine increased the maximum NA oxidation current in MA by 38% from 11.6 to 15.9 pA, whereas the current for MV was unchanged. There was a slight increase in MA constriction in the presence of cocaine; however, no change was seen in MV. The summary plots shown in Fig. 8*C* and *D* reveal that cocaine increased the oxidation current in MA at all frequencies. The largest increases ($>$ 150% of control) occurred at the lower stimulation frequencies. MA constriction increased in the presence of cocaine at frequencies up to 7 Hz, above which no change was seen. Oxidation currents or neurogenic constriction in MV were not altered significantly by cocaine at any stimulation frequency (Fig. 8*C* and *D*). Tables 1 and 2 present a statistical analysis of the NA oxidation current and contractile response data in MA and MV in the absence and presence of cocaine. Cocaine increased the rate of rise and the half-decay time of the oxidation current in MA at 3 and 20 Hz stimulation. Cocaine also increased

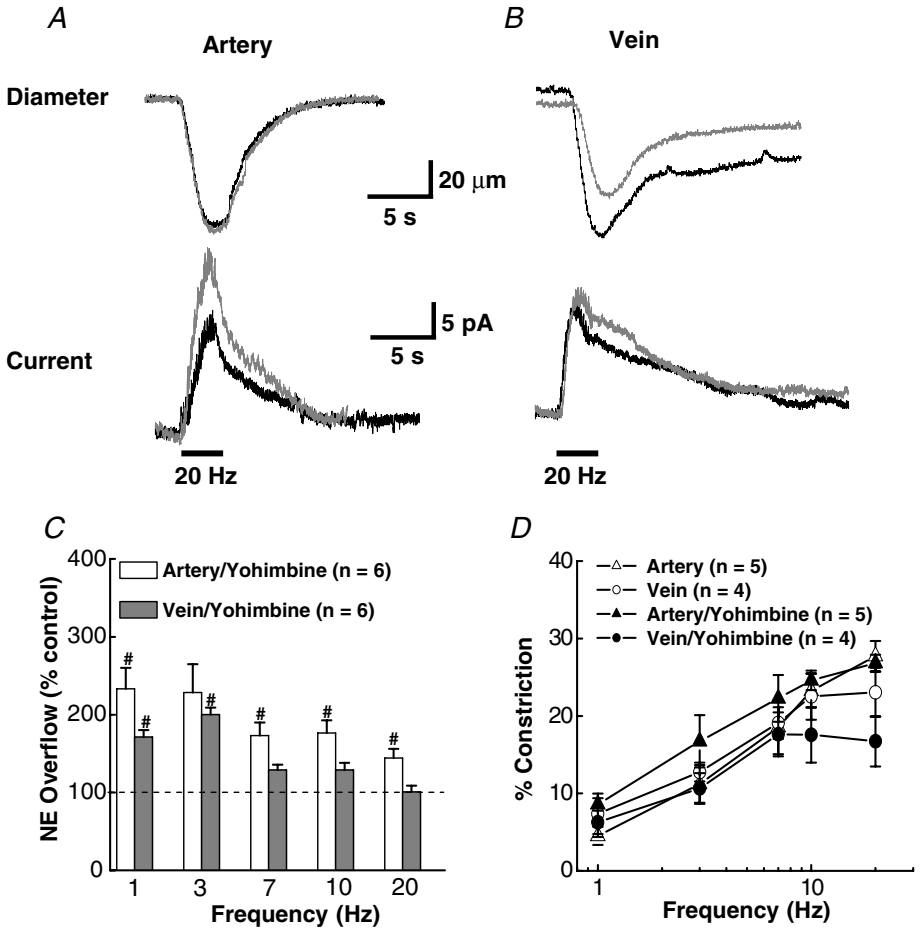

Figure 6. Effect of yohimbine on NA oxidation currents and neurogenic constriction of MA and MV
A, recordings of oxidation current and constriction in a MA in the absence and presence of yohimbine (1 μM). *B*, oxidation current and constriction in a MV with and without yohimine. Yohimbine increased the current but not constriction in MA. Yohimbine had little effect on the oxidation current in MV but it reduced the constriction. Bars under the current traces indicate the period of nerve stimulation (60 pulses, 0.3 ms pulse duration.) *C*, percentage increase in NA oxidation currents in MA and MV in the presence of yohimbine. *D*, frequency–response curves for vasoconstriction in MA and MV in the absence (control) and in the presence of yohimbine. #Significantly different from control ($P < 0.05$). Data are means ± S.E.M.

Table 1. Effects of yohimbine (1 μm), cocaine (10 μm) and cocaine with yohimbine on the time course of NA oxidation currents and constriction of mesenteric arteries

	Hz	Control ($n = 10$)	Yohimbine ($n = 4$)	Cocaine ($n = 4$)	Cocaine + Yohimbine ($n = 4$)
Current rate of rise (pA s^{-1})	3	0.05 ± 0.01	0.09 ± 0.01*	0.18 ± 0.05*	0.19 ± 0.05*
	20	0.79 ± 0.07	1.33 ± 0.17*	1.28 ± 0.28*	1.89 ± 0.32*
Current half decay (s)	3	2.85 ± 0.15	4.52 ± 1.76	6.93 ± 1.18*	9.81 ± 0.89*
	20	3.16 ± 0.34	5.04 ± 1.17	5.74 ± 1.97*	8.17 ± 1.52*
Constriction rate (mm s^{-1})	3	3.31 ± 0.92	6.54 ± 1.23	9.58 ± 0.98*	6.12 ± 0.87*
	20	21.27 ± 1.34	21.57 ± 1.08	20.94 ± 1.75	19.53 ± 1.81
Relaxation time (s)	3	7.36 ± 0.43	8.86 ± 3.29	7.85 ± 2.47	9.14 ± 2.81
	20	13.95 ± 1.37	12.1 ± 3.5	20.71 ± 3.23*	9.63 ± 2.52

Data are mean ± S.E.M. and are reported for 3 and 20 Hz stimulations. *Significant difference from control values

Table 2. Effects of yohimbine (1 μm), cocaine (10 μm) and cocaine with yohimbine on the time course of NA oxidation currents and constriction of mesenteric veins

	Hz	Control ($n = 20$)	Yohimbine ($n = 4$)	Cocaine ($n = 4$)	Cocaine + Yohimbine ($n = 4$)
Current rate of rise (pA s^{-1})	3	0.09 ± 0.01	0.15 ± 0.02*	0.24 ± 0.09*	0.14 ± 0.01*
	20	1.14 ± 0.08	1.12 ± 0.12	1.14 ± 0.32	0.82 ± 0.16
Current half decay (s)	3	3.12 ± 0.29	4.68 ± 0.59*	6.72 ± 1.54*	6.30 ± 0.77*
	20	2.70 ± 0.31	3.64 ± 0.82	2.47 ± 0.53	4.67 ± 0.94
Constriction rate (μm s^{-1})	3	12.67 ± 1.73	3.01 ± 0.40*	18.16 ± 3.94	4.43 ± 0.22*
	20	31.53 ± 2.91	13.27 ± 3.13*	20.96 ± 5.17	27.57 ± 4.09
Relaxation time (s)	3	53.20 ± 13.5	38.7 ± 7.7	116 ± 38	39.54 ± 7.87
	20	51.90 ± 9.80	19.6 ± 2.9	79.9 ± 36.4	47.63 ± 9.59

Data are mean ± S.E.M. and are reported for 3 and 20 Hz stimulations. *Significant difference from control values.

the constriction rate in MA for the 3 but not the 20 Hz stimulation, while the constriction relaxation time was prolonged only after the 20 Hz stimulation (Table 1). Cocaine increased the rate of rise of the NA oxidation current and prolonged the current half-decay time only at 3 Hz stimulation in MV. The time course of constriction was unaltered by cocaine in MV (Table 2).

In order to study the interplay between reuptake and the prejunctional α_2-adrenergic autoreceptor, cocaine (10 μM) and yohimbine (1 μM) were used together to study the combined effect on NA oxidation currents and constriction. Figure 9*A* and *B* shows constriction and oxidation currents in response to a 3 Hz train of stimuli in the absence (control) and presence of cocaine and yohimbine. Combined drug treatment increased oxidation currents in MA above the response elicited by either drug alone (Figs 6*A* and 8*A*). An increase was also observed for MV but not to the same level as MA. For example, the NA oxidation current for MA increased by 656% in the presence of both drugs (4–30 pA), whereas a smaller increase of 333% from 5 to 15 pA was seen for MV. MA constriction increased by 82% while the response for MV increased by only 8% at 3 Hz. Figure 9*C*, *D* shows plots of the oxidation currents and constriction (% of control) at different stimulation frequencies. Larger increases in oxidation current occurred in MA compared to MV particularly at low stimulation frequencies. The contractile response increased at frequencies < 7 Hz but not at high frequencies for MA, whereas the response for MV was decreased at all frequencies. The data in Table 1 show that the combined drug application significantly increased all values related to oxidation current in MA at both 3 and 20 Hz. Combined drug treatment had only a modest effect on constriction in MA (Table 1). The rate of rise of the oxidation current, current half-decay and constriction rate were increased significantly only at 3 Hz in MV in the presence of both drugs (Table 2).

Discussion

Arrangement of nerves

MA and MV are supplied by sympathetic nerves at the medial–adventitial border, but there are fewer nerve fibres in MV than in MA (Furness & Marshall, 1974; Nilsson *et al.* 1986). This does not necessarily indicate that the innervation density of MV is less than MA. MV have a thinner medial layer than MA so the number of axons per smooth muscle cell could be similar in MA and MV. This supposition is supported by the fact that ultrastructural

studies have shown that guinea pig MA and MV possess a similar density of neuromuscular junctions (Klemm *et al.* 1993). The nerve plexus for MA consists of bundles of axons arranged in a mesh-like network with nerve fibres equally likely to run parallel or perpendicular to the longitudinal axis of the vessel. For MV, the plexus consists of single axons with a circumferential nerve fibre arrangement. This arrangement made optimal detection of NA oxidation current dependent on the position of the recording microelectrode, more so than for MA. Small microelectrode movements ($\leq 50\ \mu$m) resulted in a marked change in NA oxidation current for MV. Therefore, NA oxidation current measurements were made with MV only after the electrode had been optimally positioned to record the maximum current.

In vitro continuous amperometry

Our data, and results published by other groups (Gonon *et al.* 1993; Dunn *et al.* 1999; Brock *et al.* 2000), show that NA at the blood vessel surface, caused by release from perivascular sympathetic nerve fibres, can be measured using *in vitro* continuous amperometry. The electrochemical method is particularly useful for investigating NA dynamics in real time near the sites of release. Amperometry with a microelectrode provides different

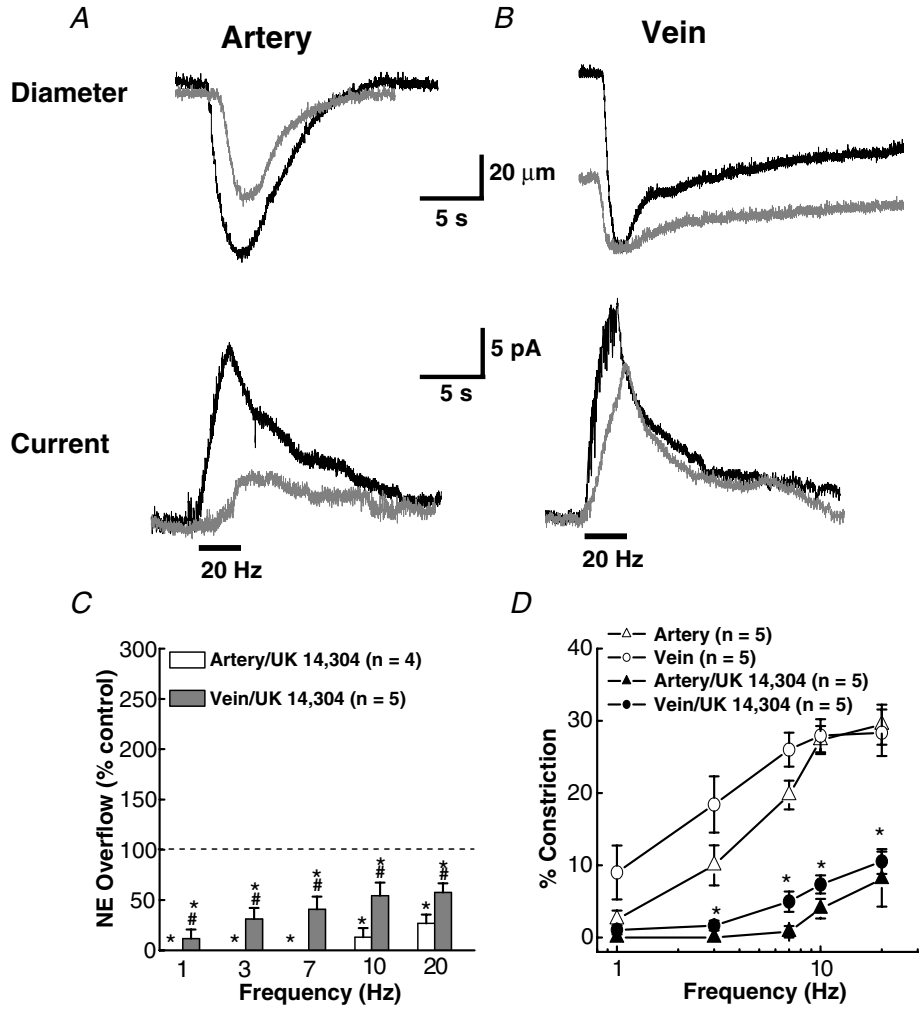

Figure 7. Effect of UK 14,304 on NA oxidation currents and neurogenic constriction of MA and MV
A, recordings of constriction (upper traces) and oxidation currents (lower traces) in a MA in the absence and presence of UK 14,304 (1 μM). UK 14,304 reduced the current and constriction. *B*, similar recordings in a MV. UK 14,304 caused a constriction of the MV but had little effect on the oxidation current. The bars under the current traces in *A* and *B* indicate the period of nerve stimulation (60 pulses with a 0.3 ms pulse width). *C*, frequency-dependent inhibition of NA oxidation currents in MA and MV by UK 14,304. Data are expressed as a percentage of the response obtained before UK 14,304. *Significantly different from control. #Significantly different from MA. *D*, frequency–response curves (1.0–20 Hz) for constriction in MA and MV in the absence (control) and presence of UK 14,304. *Significantly different from control for both MA and MV ($P < 0.05$). Data are means ± S.E.M.

information from that of more traditional spillover measurements. Amperometric recording and spillover measurements are both sensitive to the fraction of released NA that is transported away from varicosities. However, with amperometric techniques, the distance from the release site to the recording microelectrode is minimized as are the number of variables that could alter NA measurement. Spillover measurements require longer stimulus trains to evoke detectable release and reflect an NA released from large segments of blood vessels and many nerve fibres.

Postjunctional differences in neuroeffector transmission in MA and MV

Our observations that MV are more sensitive to the constricting effects of sympathetic input than MA are consistent with the literature (Kreulen, 1986; Hottenstein & Kreulen, 1987; Luo *et al.* 2003). There are several mechanisms that contribute to the differences in neuroeffector transmission in MA and MV.

Firstly, the transmitters released from periarterial and perivenous sympathetic nerves contribute to the functional differences in MA and MV. The α_1-adrenergic receptor antagonist, prazosin, had a minor effect on neurogenic constriction of MA but it blocked MV constriction. On the other hand, the P2X receptor antagonist, PPADS, largely blocked constriction in MA but not in MV. These observations are consistent with neurogenic constrictions in MV being mediated by NA acting at α_1-adrenergic receptors, and by ATP acting at $P2X_1$ purinergic receptors in small MA, particularly at low stimulation frequencies (Smyth *et al.* 2000; Galligan *et al.* 2001; Gitterman & Evans, 2001; Luo *et al.* 2003).

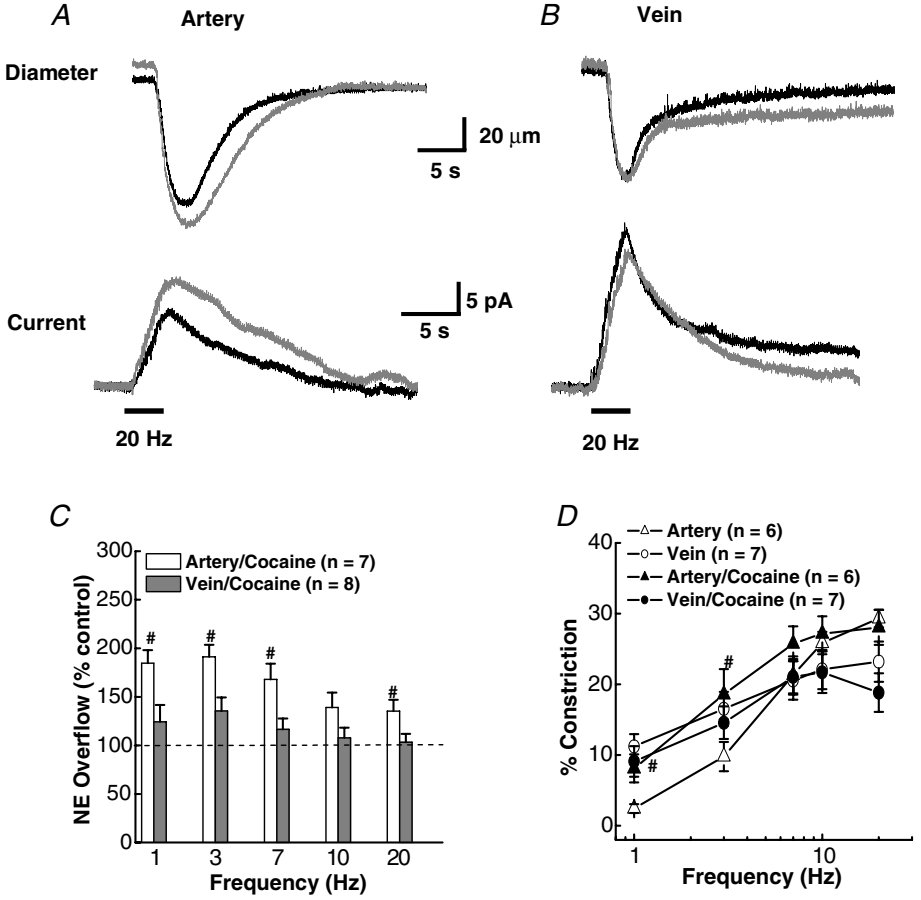

Figure 8. Effect of cocaine on NA oxidation current and neurogenic constriction in of MA and MV
A, representative recordings of constriction (upper traces) and oxidation currents (lower traces) in a MA in the absence and presence of cocaine (10 μM). Cocaine increased the current but had little effect on the constriction. *B*, similar recordings in a MV. Cocaine did not change the NA oxidation current or constriction in MV. The bars under the current traces in *A* and *B* indicate the period of nerve stimulation (60 pulses with a 0.3 ms pulse width). *C*, frequency-dependent increase in the NA oxidation current in MA but not MV by cocaine. Data are of expressed as a percentage of the response obtained before cocaine treatment in each tissue. #Significantly different from control levels. *D*, frequency–response curves (1.0–20 Hz) for vasoconstriction in MA and MV in the absence (control) and in the presence of cocaine. #Significantly different from control levels for both MA ($P < 0.05$). Cocaine did not change constriction in MV at any stimulation frequency. Data are means ± S.E.M.

Second, there are kinetic differences in the neurogenic constrictions of MA and MV. The kinetics of vascular constriction are determined by the spatio-temporal pattern of neurotransmitter release and clearance, post-receptor signalling, density of innervation and the width of neuromuscular cleft (Gonon *et al.* 1993; Kreulen, 2003*b*). The constriction rate is faster in MV than in MA. The predominant constrictor in MA is ATP acting at $P2X_1$ receptors, which are ligand-gated cation channels (North, 2000). The predominant constrictor in MV is NA acting at α_1-adrenergic receptors, which are G-protein coupled receptors (Wier & Morgan, 2003). The faster rate of venous constriction could be related to the different signalling mechanisms used by $P2X_1$ receptors that use extracellular calcium to cause MA contraction (Gitterman & Evans, 2001) and α_1-adrenergic receptors that mobilize intracellular calcium and alter the phosphorylation state of contractile proteins (Kitazawa *et al.* 2000). The faster rate of venous constriction might also involve selective activation of postjunctional α_2-adrenergic receptors in MV. Selective expression of functional postjunctional α_2-adrenergic receptors in MV might also contribute to the greater sensitivity of MV to the constrictor effects of endogenously released NA. Using a microelectrode calibration procedure that mimics neurogenic release, we determined the apparent NA concentration caused by the efflux from nearby varicosities. This permitted comparison of endogenous NA concentration–response

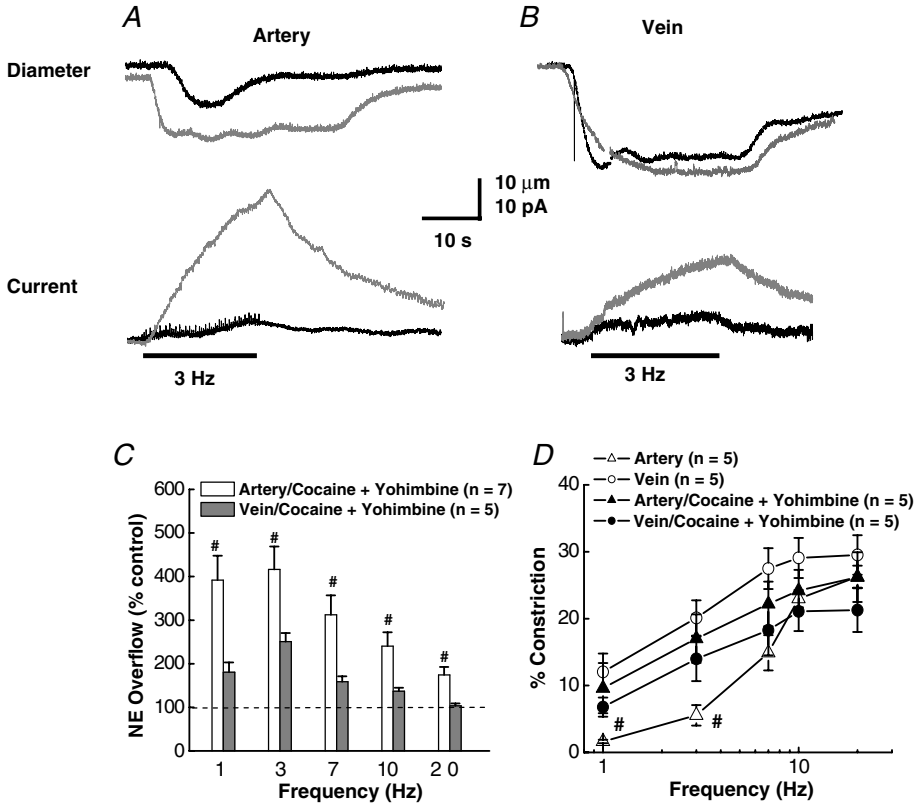

Figure 9. Effects of combined inhibition of NET and α_2 autoreceptors on NA oxidation currents and constrictions of MA and MV

A, representative recordings of constriction (upper traces) and current (lower traces) caused by a 3 Hz train of stimulation of a MA in the absence and presence of cocaine (10 μM) and yohimbine (1 μM). *B*, representative recordings of constriction (upper traces) and current (lower traces) caused by a 3 Hz train of stimulation in a MV in the absence and presence of cocaine (10 μM) and yohimbine (1 μM). Combined drug application increased the current response in MA and MV but the drugs increased constriction only in MA. *C*, frequency–response curves (1–20 Hz, 60 pulses) for cocaine/yohimbine induced increases in NA oxidation currents in MA and MV. Combined drug application increased NA oxidation currents in MA at low frequencies (< 7 Hz) but did not change significantly the oxidation currents in MV. Data are expressed as a percentage increase in oxidation currents over values obtained in the same blood vessels before drug application. #Significantly different from control values ($P < 0.05$). *D*, frequency–response curves for neurogenic constriction of MA and MV in the absence and presence of combined application of cocaine and yohimbine. Combined drug application increased MA constrictions at 1 and 3 Hz. #Significantly different from control values ($P < 0.05$). Constrictions of MV were not significantly affected by combined drug application. Data are means ± S.E.M.

curves in the two vessel types. MA was less sensitive than MV to the constrictor effects of endogenously released NA. These data are consistent with previously published work (Luo *et al.* 2003) showing that MV are more sensitive to the constrictor effects of exogenous NA.

Prejunctional differences in neuroeffector transmission in MA and MV

Frequency–response curves for the NA oxidation currents measured at the surface of MV were left-shifted from those for MA. Similar findings were obtained in NA spillover studies from whole MA and MV segments, assessed by high-performance liquid chromatography (HPLC) (Smyth *et al.* 2000; Bobalova & Mutafova-Yambolieva, 2001). In both cases, the increased NA overflow in MV relative to MA could be caused by several factors.

Firstly, the mechanisms of NA release from perivenous and periarterial sympathetic nerves could differ such that individual action potentials release more NA in MV. There are no data available to address this issue; however, different populations of sympathetic nerves are known to supply arteries and veins (Browning *et al.* 1999; Hsieh, 2000).

Secondly, there may be differential expression of α_2-autoreceptors by arterial and venous sympathetic nerves. Prejunctional α_2-adrenergic autoreceptors located at the sympathetic nerve terminals are activated following exocytotic release of NA and inhibit further release (Langer, 1980). The absence or blockade of the autoreceptor would lead to less regulated release and higher junctional concentrations of NA. Blocking α_2-adrenergic receptors with yohimbine increased peak NA oxidation currents in MA at all stimulation frequencies. The key role prejunctional α_2 autoreceptors play in modulating NA release from sympathetic nerves supplying rat mesenteric arteries has been reported previously (Dunn *et al.* 1999). Oxidation currents in MV were increased by yohimbine only at low stimulation frequencies. Yohimbine also increased the rate of rise of the NA oxidation current in MA at 3 and 20 Hz in MA but it increased the rate of rise of the oxidation current in MV at 3 Hz only. These data indicate that NA release rate is tightly coupled to prejunctional autoreceptors in MA but less so in MV. We also found that UK 14,304 decreased NA oxidation currents in MA and MV, but this effect was larger in MA. Taken together these data indicate that prejunctional α_2-adrenergic autoreceptors play a more prominent role in regulating NA release in MA than in MV. The reduced influence of α_2 autoreceptors in MV may be due to differences in autoreceptor density or spatial separation from release sites.

Thirdly, differences in NA oxidation currents in MA and MV might be due to differences in clearance efficiency. Termination of the action of NA at the neuroeffector junction depends on removal from the neuroeffector junction by NET and low affinity extraneuronal cation transporters, and by metabolism and diffusion (Eisenhofer, 2001). Therefore, the junctional concentration of NA and its postjunctional effect are influenced by release dynamics, reuptake, metabolism and diffusion (Esler *et al.* 1990). Most estimates indicate that 90% of released NA is transported back into the nerve terminal *via* NET so other mechanisms play only a minor role in NA clearance. The NA that escapes recovery by NET is what is detected by the microelectrode. Therefore, the measured NA concentration is lower than the true junctional concentration (Mermet *et al.* 1990; Gonon *et al.* 1993; Dunn *et al.* 1999), but nonetheless reflects the release and clearance processes. We found that inhibition of NET by cocaine increased measured NA in MA preparations. Similar results have been obtained previously in studies using desmethylimipramine to block NET in rat mesenteric arteries (Dunn *et al.* 1999). In contrast, cocaine had relatively little effect on NA oxidation currents in MV. These data indicate that NET is an important determinant of NA concentrations in the junctional cleft in MA while diffusion or metabolism are more important for clearance in MV.

Combined application of cocaine and yohimbine produced a modest increase in NA oxidation currents in MV preparations without increasing constriction at frequencies > 7 Hz. In some cases, constriction actually decreased with the combined drugs. The unchanging constriction maximum is likely to be due to saturation of the postjunctional receptors on the vascular smooth muscle cells due to the prolonged presence of high junctional NA concentrations.

Summary and conclusions

The data presented herein indicate that the time-dependent concentration of NA at artery and vein surfaces, caused by complex mechanisms of release and clearance at sympathetic varicosities, can be studied *in vitro* using continuous amperometry. The key finding from this work is that differential neurogenic control of MA and MV was demonstrated. These differences include, arrangement of perivascular nerve fibres, neurotransmitters mediating constriction, sensitivity to the constrictor effects of endogenous NA, function of the α_2-autoreceptor and NET. MA are much less sensitive to the constrictor effects of endogenously released NA than are MV. NA release and clearance in the arterial neuroeffector junction is tightly regulated by α_2-adrenergic autoreceptors and NET. While α_2-adrenergic autoreceptors regulate NA release at the perivenous neuroeffector junction, this effect is

less prominent than in arteries. NA makes only a minor contribution of neurogenic constriction of MA under our experimental conditions even though it is released in both MA and MV. NA, acting at prejunctional α_2 autoreceptors, may function as a modulator of ATP release in small MA. A similar conclusion has been reached by previous investigators who studied sympathetic neuroeffector transmission in guinea pig small intestinal submucosal arterioles (Evans & Surprenant, 1992). NET contributes little to NA clearance at the venous neuroeffector junction. These differences in neuroeffector transmission may contribute to the different haemodynamic functions of arteries and veins. Rapidly developing and sustained constrictions of veins are required to offset orthostatic changes in blood distribution while phasic changes in arterial tone would facilitate moment to moment blood pressure control and organ perfusion.

References

Bjorklund A, Lindvall O & Svensson LA (1972). Mechanisms of fluorophore formation in the histochemical glyoxylic acid method for monoamines. *Histochemie* **32**, 113–131.

Bobalova J & Mutafova-Yambolieva VN (2001). Presynaptic α2-adrenoceptor-mediated modulation of adenosine 5′-triphosphate and noradrenaline corelease: differences in canine mesenteric artery and vein. *J Auton Pharmacol* **21**, 47–55.

Brock JA, Dunn WR, Boyd NSF & Wong DKY (2000). Spontaneous release of large packets of noradrenaline from sympathetic nerve terminals in rat mesenteric arteries in vitro. *Br J Pharmacol* **131**, 1507–1511.

Brock JA & Tan JH (2004). Selective modulation of noradrenaline release by α_2-adrenoceptor blockade in the rat-tail artery in vitro. *Br J Pharmacol* **142**, 267–274.

Browning K, Zheng Z, Kreulen D & Travagli R (1999). Two populations of sympathetic neurons project selectively to mesenteric artery or vein. *Am J Physiol Heart Circ Physiol* **276**, H1263–H1272.

Chow RH, von Ruden L & Neher E (1992). Delay in vesicle fusion revealed by electrochemical monitoring of single secretory events in adrenal chromaffin cells. *Nature* **356**, 60–63.

Daugirdas JT (2001). Pathophysiology of dialysis hypotension: an update. *Am J Kidney Dis* **38**, S11–S17.

Dugast C, Cespuglio R & Suaud-Chagny MF (2002). In vivo monitoring of evoked noradrenaline release in the rat anteroventral thalamic nucleus by continuous amperometry. *J Neurochem* **82**, 529–537.

Dunn WR, Brock JA & Hardy TA (1999). Electrochemical and electrophysiological characterization of neurotransmitter release from sympathetic nerves supplying rat mesenteric arteries. *Br J Pharmacol* **128**, 174–180.

Eisenhofer G (2001). The role of neuronal and extraneuronal plasma membrane transporters in the inactivation of peripheral catecholamines. *Pharmacol Ther* **91**, 35–62.

Esler M, Jennings G, Lambert G, Meredith I, Horne M & Eisenhofer G (1990). Overflow of catecholamine neurotransmitters to the circulation: source, fate, and functions. *Physiol Rev* **70**, 963–985.

Evans RJ & Surprenant A (1992). Vasoconstriction of guinea-pig submucosal arterioles following sympathetic nerve stimulation is mediated by the release of ATP. *Br J Pharmacol* **106**, 242–249.

Furness JB & Marshall JM (1974). Correlation of the directly observed responses of mesenteric vessles of the rat to nerve stimulation and noradrenaline with the distribution of adrenergic nerves. *J Physiol* **239**, 75–88.

Galligan JJ, Hess MC, Miller SB & Fink GD (2001). Differential localization of P2 receptor subtypes in mesenteric arteries and veins of normotensive and hypertensive rats. *J Pharmacol Exp Ther* **296**, 478–485.

Gitterman DP & Evans RJ (2001). Nerve evoked P2X receptor contractions of rat mesenteric arteries; dependence on vessel size and lack of role of L-type calcium channels and calcium induced calcium release. *Br J Pharmacol* **132**, 1201–1208.

Gonon F (1995). Monitoring dopamine and noradrenaline release in central and peripheral nervous systems with treated and untreated carbon-fiber electrodes. *Neuromethods* **27**, 153–177.

Gonon F, Bao JX, Msghina M, Suaud-Chagny MF & Stjärne L (1993). Fast and local electrochemical monitoring of noradrenaline release from sympathetic terminals in isolated rat tail artery. *J Neurochem* **60**, 1251–1257.

Gonon F, Msghina M & Stjärne L (1993). Kinetics of noradrenaline released by sympathetic nerves. *Neuroscience* **56**, 535–538.

Hirst GD & Jobling P (1989). The distribution of γ-adrenoceptors and P2 purinoceptors in mesenteric arteries and veins of the guinea-pig. *Br J Pharmacol* **96**, 993–999.

Hottenstein OD & Kreulen DL (1987). Comparison of the frequency dependence of venous and arterial responses to sympathetic nerve stimulation in guinea-pigs. *J Physiol* **384**, 153–167.

Hsieh NK, Liu JC & Chen HI (2000). Localization of sympathetic postganglionic neurons innervating mesenteric artery and vein in rats. *J Auton Nerv Syst* **80**, 1–7.

Kitazawa T, Eto M, Woodsome TP & Brautigan DL (2000). Agonists trigger G protein-mediated activation of the CPI-17 inhibitor phosphoprotein of myosin light chain phosphatase to enhance vascular smooth muscle contractility. *J Biol Chem* **275**, 9897–9900.

Klemm MF, Van Helden DF & Luff SE (1993). Ultrastructural analysis of sympathetic neuromuscular junctions on mesenteric veins of the guinea pig. *J Comp Neurol* **334**, 159–167.

Kreulen DL (1986). Activation of mesenteric arteries and veins by preganglionic and postganglionic nerves. *Am J Physiol Heart Circ Physiol* **251**, H1267–H1275.

Kreulen DL (2003*a*). Properties of the venous and arterial innervation in the mesentery. *J Smooth Muscle Res* **39**, 269–279.

Kreulen DL (2003*b*). Properties of the venous and arterial innervation in the mesentery. *J Smooth Muscle Res* **39**, 269–279.

Langer SZ (1980). Presynaptic regulation of the release of catecholamines. *Pharmacol Rev* **32**, 337–362.

Luo M, Hess MC, Fink GD, Olson LK, Rogers J, Kreulen DL, Dai X & Galligan JJ (2003). Differential alterations in sympathetic neurotransmission in mesenteric arteries and veins in DOCA-salt hypertensive rats. *Auton Neurosci* **104**, 47–57.

Mermet C, Gonon FC & Stjärne L (1990). On-line electrochemical monitoring of the local noradrenaline release evoked by electrical stimulation of the sympathetic nerves in isolated rat tail artery. *Acta Physiol Scand* **140**, 323–329.

Nilsson H, Goldstein M, Nilsson O, Ljung B, Sjoblom N & Wallin BG (1986). Adrenergic innervation and neurogenic response in large and small arteries and veins from the rat. *Acta Physiol Scand* **126**, 121–133.

North RA & Suprenant A (2000). Pharmacology of cloned P2X receptors. *Annu Rev Pharmacol Toxicol* **40**, 563–580.

Park J, Galligan JJ, Fink GD & Swain GM(2006*a*). In vitro continuous amperometry with a diamond microelectrode coupled with video microscopy for simultaneously monitoring endogeneous norepinephrine and its effect on the contractile response of a rat mesenteric artery. *Anal Chem* **78**, 6756–6766.

Park J, Quaiserová-Mocko V, Pecková K, Galligan JJ, Fink GD & Swain GM (2006*b*). Fabrication, characterization, and application of a diamond microelectrode for electrochemical measurement of norepinephrine release from the sympathetic nervous system. *Diamond Relat Mater* **15**, 761–772.

Park J, Show Y, Quaiserova V, Galligan JJ, Fink GD & Swain GM (2005). Diamond microelectrodes for use in biological environments. *J Electroanal Chem* **583**, 56–68.

Ranganathan S, Kuo T-C & McCreery RL (1999). Facile preparation of active glassy carbon electrodes with activated carbon and organic solvents. *Anal Chem* **71**, 3574–3580.

Segal SS (2000). Integration of blood flow control to skeletal muscle: key role of feed arteries. *Acta Physiol Scand* **168**, 511–518.

Smyth L, Bobalova J, Ward SM, Keef KD & Mutafova-Yambolieva VN (2000). Cotransmission from sympathetic vasoconstrictor neurons: differences in guinea-pig mesenteric artery and vein. *Auton Neurosci* **86**, 18–29.

Stamford JA (1986). In vivo voltammetry: some methodological considerations. *J Neurosci Methods* **17**, 1–29.

Stjarne L, Bao JX, Gonon F & Msghina M (1994*a*). Nerve activity-dependent variations in clearance of released noradrenaline: regulatory roles for sympathetic neuromuscular transmission in rat tail artery. *Neuroscience* **60**, 1021–1038.

Stjarne L, Astrand P, Bao JX, Gonon F, Msghina M & Stjarne E (1994*b*). Spatiotemporal pattern of quantal release of ATP and noradrenaline from sympathetic nerves: consequences for neuromuscular transmission. *Adv Second Messenger Phosphoprotein Res* **29**, 461–496.

Tani H, Singer W, McPhee BR, Opfer-Gehrking TL, Haruma K, Kajiyama G & Low PA (2000). Splanchnic-mesenteric capacitance bed in the postural tachycardia syndrome (POTS). *Auton Neurosci* **86**, 107–113.

Teschemacher AG (2005). Real-time measurements of noradrenaline release in periphery and central nervous system. *Auton Neurosci* **117**, 1–8.

Westfall DP, Todorov LD & Mihaylova-Todorova ST (2002). ATP as a cotransmitter in sympathetic nerves and its inactivation by releasable enzymes. *J Pharmacol Exp Ther* **303**, 439–444.

Westfall TC, Yang CL, Rotto-Perceley D & Macarthur H (1996). Neuropeptide Y–ATP interactions and release at the vascular neuroeffector junction. *J Auton Pharmacol* **16**, 345–348.

Wier WG & Morgan KG (2003). α_1-Adrenergic signaling mechanisms in contraction of resistance arteries. *Rev Physiol Biochem Pharmacol* **150**, 91–139.

Yavich L, Jakala P & Tanila H (2005). Noradrenaline overflow in mouse dentate gyrus following locus coeruleus and natural stimulation: real-time monitoring by in vivo voltammetry. *J Neurochem* **95**, 641–650.

Zhou Z & Misler S (1996). Amperometric detection of quantal secretion from patch-clamped rat pancreatic β-cells. *J Biol Chem* **271**, 270–277.

Acknowledgements

This research was supported by grants from the National Institutes of Health, HL63973 and HL70687 (G.D.F. and J.J.G.), and HL84258 (G.M.S.).